

To be submitted to the *Astrophysical Journal*

## The Molecular Line Opacity of MgH in Cool Stellar Atmospheres

P. F. Weck, A. Schweitzer, P. C. Stancil & P. H. Hauschildt

*Department of Physics and Astronomy and Center for Simulational Physics,  
The University of Georgia, Athens, GA 30602-2451*

weck@-,andy@-,stancil@-,yeti@physast.uga.edu

K. Kirby

*Harvard-Smithsonian Center for Astrophysics  
60 Garden St., Cambridge, MA 02138*

kirby@cfa.harvard.edu

### ABSTRACT

A new, complete, theoretical rotational and vibrational line list for the  $A \ ^2\Pi \leftarrow X \ ^2\Sigma^+$  electronic transition in MgH is presented. The list includes transition energies and oscillator strengths for all possible allowed transitions and was computed using the best available theoretical potential energies and dipole transition moment function with the former adjusted to account for experimental data. The  $A \leftarrow X$  line list, as well as new line lists for the  $B' \ ^2\Sigma^+ \leftarrow X \ ^2\Sigma^+$  and the  $X \ ^2\Sigma^+ \leftarrow X \ ^2\Sigma^+$  (pure rovibrational) transitions, were included in comprehensive stellar atmosphere models for M, L, and T dwarfs and solar-type stars. The resulting spectra, when compared to models lacking MgH, show that MgH provides significant opacity in the visible between 4400 and 5600Å . Further, comparison of the spectra obtained with the current line list to spectra obtained using the line list constructed by Kurucz (1993a) show that the Kurucz list significantly overestimates the opacity due to MgH particularly for the bands near 5150 and 4800Å with the discrepancy increasing with decreasing effective temperature.

*Subject headings:* molecular data — stars: atmospheres — stars: late-type

## 1. Introduction

The study of the spectra of cool stars requires detailed knowledge of molecular opacities. This includes important absorbers such as TiO, CO, and water vapor, which have bands that cover large wavelength ranges and are very important for the structure of the atmosphere due to their overall cooling or heating effects.

In addition, there are a number of molecules that have bands covering comparatively small wavelength ranges (e.g., a few 10 or 100 Å). Many of them are trace molecules that have only small effects on the overall physical conditions inside the atmosphere but that are important for spectral classification and for the determination of stellar parameters such as effective temperatures, gravities and abundances. Unfortunately, important molecular data such as energy levels, bound-free, and bound-bound cross-sections are only poorly known or not known at all for a number of these trace molecules. We have therefore started a project to update or provide for the first time molecular data of astrophysical interest for important trace molecules and consider in this work MgH. These data will be computed using state-of-the-art molecular physics codes and should improve our ability to model and analyze cool stellar atmospheres considerably.

It is important to assess the quality of the computed molecular data. This is best done by comparing to experimental results; however, this is only possible for very few molecules of astrophysical interest. In addition, in many cases the temperature range of astrophysical importance is higher than what can be reached with current experimental setups. Therefore, indirect methods of testing and evaluating the molecular data are useful. In this paper, we use the general-purpose stellar atmosphere code PHOENIX to calculate model atmospheres and synthetic spectra with and without the new molecular data. The results of these calculations can then be used to assess the importance of particular molecular opacities on the structure of the atmosphere. The synthetic spectra can be used to verify the correct strength of the computed bands when compared to observational data. This procedure introduces uncertainties such as the treatment of the equation of state (e.g., the molecular data used in it), the treatment of lines and line profiles and the assumed parameters of the comparison star. However, differential analyses circumvent many of these problems and should allow a reasonable evaluation of the molecular bound-free and free-free data.

The electronic bands of magnesium hydride have been detected over a wide range of stellar atmospheres including the photosphere of the sun (Sotirovski 1972), sunspot umbrae (Wallace et al. 1999), F-K giants in the Milky Way halo and halos of other Local Group galaxies (Majewski et al. 2000), and nearby L-dwarfs (Reid et al. 2000). MgH lines can be used as indicators of surface gravity in late-type stars (Bonnell & Bell 1993) and to determine magnesium isotope abundances (Wallace et al. 1999; Gay & Lambert 2000).

The spectrum of MgH has been extensively studied in the laboratory for many decades (Balfour & Cartwright 1976; Balfour & Lindgren 1978; Bernath et al. 1985; Wallace et al. 1999, and references therein) and has received some theoretical attention (Saxon et al. 1978; Kirby et al. 1979, and references therein). However, modern stellar atmosphere calculations require extensive, and complete, molecular line lists as molecular band absorption is the primary source of line-blanketing in cool stellar atmospheres, particularly M dwarfs. For many molecules, including MgH, the only source for complete line lists is the extensive compilations of Kurucz (1993a). While these compilations are highly valuable to stellar modelers, the methods necessary to compute 100s of millions of lines require a number of approximations which at times are severe. In this work, we apply fully quantum-mechanical techniques to compute the complete line list for the  $A\ ^2\Pi \leftarrow X\ ^2\Sigma^+$  transition of MgH. The parameters of the calculation are adjusted to force agreement with available experiments. However, our goal is to reproduce the global MgH opacity, hence we cannot claim spectroscopic accuracy for a particular line. The  $A \leftarrow X$  line list constructed in this work is combined with line lists for the  $B'\ ^2\Sigma^+ \leftarrow X\ ^2\Sigma^+$  and the  $X\ ^2\Sigma^+ \leftarrow X\ ^2\Sigma^+$  transitions computed by Skory et al. (2002) and tested in a range of stellar atmosphere models. An overview of the theory of molecular rotational lines is presented in section 2 with the results of the line list calculations and stellar models are given in section 3. We present our conclusions in section 4.

## 2. Molecular theory

### 2.1. Potential curves and dipole transition moments

For the purpose of the present calculations, accurate *ab initio* potential-energy surfaces given by Saxon et al. (1978) have been used for both the  $A\ ^2\Pi$  and  $X\ ^2\Sigma^+$  electronic states of MgH. Their configuration interaction treatment includes singly- to triply-excited configurations (SDTCI) in a large Slater-type basis set, leading to good agreement of the derived spectroscopic constants with experimental data.

In order to bring the calculated potential curves into better agreement with experiment, shifts of  $+8.740 \times 10^{-4}$  a.u.<sup>1</sup> and  $-3.3665 \times 10^{-3}$  a.u. have been applied in the present work to the Saxon et al. (1978)  $X\ ^2\Sigma^+$  and  $A\ ^2\Pi$  energies, respectively. Details about this procedure are given in a separate publication for the  $B' \leftarrow X$  electronic transition in MgH (Skory et al. 2002). In this way, the dissociation energies  $D_0^0$  coincide with the experimental values given by Balfour & Lindgren (1978) for the ground state and by Balfour & Cartwright (1976)

---

<sup>1</sup>Atomic units are used throughout this section unless otherwise stated.

for the  $A\ ^2\Pi$  state. The dissociation energies adopted here are 10,243.26 and 12,903.71  $\text{cm}^{-1}$  for the  $X\ ^2\Sigma^+$  and  $A\ ^2\Pi$  of  $^{24}\text{MgH}$ , respectively. The relative energies between the two potential curves were further shifted to match the energy difference corresponding to the pure  $(0,0)$  vibronic transition. The value of  $T_0 = 19278.13\ \text{cm}^{-1}$ , which corresponds to the average of the  $Q_1(0)$  and  $Q_2(1)$  transition energies measured by Balfour & Cartwright (1976), was adopted. We note that this value for  $T_0$  does not agree with the more recent measurements of Bernath, Black, & Brault (1985) who find  $T_0 = 19284.65\ \text{cm}^{-1}$ , though it is unclear how their value was arrived at. In fact, their assumption of a Hund’s coupling case (a) is in obvious contradiction with the small and regular  $\Lambda$ -doubling parameters,  $p_0 = 0.0258\ \text{cm}^{-1}$  and  $q_0 = 0.00178\ \text{cm}^{-1}$ . Such a case for a  $^2\Pi \leftarrow ^2\Sigma^+$  transition is more typically characterized by Hund’s case (b) (Herzberg 1950, Figures 122 and 124). Further, (Bernath et al. 1985) suggest that a number of low- $J$  lines, presumably  $P_1(1)$ ,  $R_2(1)$ ,  $Q_2(0)$ ,  $Q_2(1)$ ,  $Q_2(2)$ , and  $P_2(2)$ , measured by Balfour & Cartwright (1976) do not exist apparently assuming Hund’s case (a). However, we find that under Hund’s case (b) all but  $P_1(1)$  and  $Q_2(0)$  do in fact exist. We therefore adopted the value of  $T_0$  deduced from Balfour & Cartwright (1976).

Out of the range of internuclear separations  $R = 2.2\ a_o$  to  $9.5\ a_o$  considered by Saxon et al. (1978), the potential curves have been extrapolated in two different ways. On the one hand, for internuclear distances  $R > 9.5\ a_o$ , a smooth fit to the *ab initio* potentials has been performed using the average long-range interaction potential

$$V_L(R) = -\frac{C_6}{R^6} - \frac{C_8}{R^8} - \frac{C_{10}}{R^{10}}, \quad (1)$$

where  $C_6$ ,  $C_8$  and  $C_{10}$  are the usual van der Waals coefficients corresponding to the dipole-dipole, dipole-quadrupole, and the sum of dipole-quadrupole and dipole-octupole interactions, respectively. For the  $X\ ^2\Sigma^+$  ground state, the coefficients described in Skory et al. (2002) were adopted as summarized in Table 1. Since to our knowledge, no data have been reported for the van der Waals constants of the  $A\ ^2\Pi$  state of  $\text{MgH}$ , they were estimated using a technique based on the London formula as described for the  $B'\ ^2\Sigma^+$  state by Skory et al. (2002). On the other hand, for internuclear distances  $R < 2.2\ a_o$ , the potential curves of both the  $X\ ^2\Sigma^+$  and the  $A\ ^2\Pi$  electronic states have been fitted to the short-range interaction exponential form  $A \exp(-BR) + C$ .

In a similar way, the dipole transition moment for  $A\ ^2\Pi \leftarrow X\ ^2\Sigma^+$  and the dipole moment of the  $X$  state calculated by Saxon et al. (1978) have been used over the range  $R = 2.2\ a_o$  to  $9.5\ a_o$ , and extrapolated by an exponential fit for both the short- and long-range interactions. The dipole transition moment and the dipole moment were both smoothly forced to zero at the united-atom and separated-atom limits.

## 2.2. Rotational and band oscillator strengths

Throughout the present study, we have adopted the now well established point of view expressed by Whiting & Nicholls (1974) with respect to the preferred way in which dipole matrix elements of a rotational transition should be separated into rotational and electronic-vibrational parts.

For the  $A \ ^2\Pi \leftarrow X \ ^2\Sigma^+$  absorption band system of the present study, the rotational oscillator strength can be expressed as given by Larsson (1983),

$$f_{v'J',v''J''}^{ab} = \frac{2}{3} \Delta E_{v'J',v''J''} \frac{S_{J'}(J'')}{2J'' + 1} |D_{v'J',v''J''}^{AX}|^2, \quad (2)$$

where  $D_{v'J',v''J''}^{AX} = \langle \chi_{v'J'} | D^{AX}(R) | \chi_{v''J''} \rangle$  is the rovibrational matrix element of the electric dipole transition moment  $D^{AX}(R)$  responsible for absorption from the  $X \ ^2\Sigma^+$  into the  $A \ ^2\Pi$  electronic state and  $\chi_{vJ}$  are the rovibrational wave functions. The Hönl-London factors  $S_{J'}(J'')$  are defined according to Whiting & Nicholls (1974) as

$$S_{J'}(J'') = \begin{cases} (J'' - 1)/2, & J' = J'' - 1 \text{ (P-branch)} \\ (2J'' + 1)/2, & J' = J'' \text{ (Q-branch)} \\ (J'' + 2)/2, & J' = J'' + 1 \text{ (R-branch)}. \end{cases} \quad (3)$$

For the sake of comparison with the band oscillator strength values calculated by Kirby et al. (1979), we used the following relation between band and rotational oscillator strengths, as defined in Eq.(2),

$$\begin{aligned} f_{v'v''}^{ab} &= \frac{1}{g_{J',J''}^{ab} S_{J'}(J'')} f_{v'J',v''J''}^{ab} \\ &= \frac{(2 - \delta_{0,\Lambda''+\Lambda'}) (2J'' + 1)}{(2 - \delta_{0,\Lambda''}) S_{J'}(J'')} f_{v'J',v''J''}^{ab}, \end{aligned} \quad (4)$$

where  $g_{J',J''}^{ab}$  is a degeneracy factor arising from spin-splitting and  $\Lambda$ -doubling in both final and initial electronic states.

## 3. Results and discussion

### 3.1. The $A - X$ rovibrational line list

The energy levels together with the rovibrational wavefunctions  $\chi_{v'J'}(R)$  and  $\chi_{v''J''}(R)$  of the final and initial electronic state have been calculated by solving the radial nuclear

equation by standard Numerov techniques (Cooley 1961). These calculations have been performed using a step of  $1 \times 10^{-3}$  a.u. for the integration over internuclear distances from  $R = 0.5$  a.u. to 200 a.u. For  $^{24}\text{MgH}$ , the reduced mass  $0.9671852 \text{ u}^2 = 1763.064$  a.u. (Huber & Herzberg 1979) was adopted.

In Table 2, the vibrational binding energies of the  $A \ ^2\Pi$  state calculated for the present study are given together with the corresponding values of  $\Delta G(v' + 1/2) = G(v' + 1) - G(v')$ . The latter are found to be in excellent agreement with the previous calculations of Saxon et al. (1978) up to  $v' = 4$ . For higher vibrational levels, a maximum difference of  $125 \text{ cm}^{-1}$  occurs for  $v' = 8$ . Moreover, our fitting procedure to the long-range interaction potential yields an additional vibrational level near threshold to give  $v'_{\text{max}} = 13$ . The maximum  $J'$  for each  $v'$  is also shown in Table 2 giving a total of 435 rovibrational states.<sup>3</sup> Comparison to the limited experimental data shows the calculated  $\Delta G$ 's to be smaller by up to  $45 \text{ cm}^{-1}$  which suggests that the Saxon et al. (1978) potential is somewhat broader than reality.

The band oscillator strength values for the band system  $A \ ^2\Pi \leftarrow X \ ^2\Sigma^+$  are given in Table 3 for the transitions between the vibrational states  $v'' = 0 - 3$  and  $v' = 0 - 6$ . The current calculations satisfactorily reproduce the theoretical results of Kirby et al. (1979).

Figure 1 shows the line absorption rotational oscillator strengths<sup>4</sup> for the  $A \ ^2\Pi \leftarrow X \ ^2\Sigma^+$  transition as a function of the energy of the absorbed photon. It is worth noting the presence of a series of peaks which correspond to the  $J' = 1 \leftarrow J'' = 0$  lines of the R-branch [ $R(0)$ ] whose intensities are larger by a factor two than all other lines in the same wavelength region. A detailed examination of the wavelength distribution of these peaks reveals that they are to be classified into three categories, according to whether they are  $\Delta v = v' - v'' = +1, 0$  or  $-1$  transitions as shown in Figure 1. Apart from these peaks, the R-branch contribution dominates over the wavelength ranges  $19,800 - 20,300 \text{ cm}^{-1}$  and  $21,050 - 21,300 \text{ cm}^{-1}$ . Other lines observed in Figure 1 are to be assigned mainly to the Q-branch transitions, which are about two times more intense than the P-branch over the whole wavelength range considered. However, the P-branch appears to play a major role for the energy range  $19,170 - 19,280 \text{ cm}^{-1}$  and  $20,450 - 20,690 \text{ cm}^{-1}$ .

The product  $g_{J',J''} \cdot f_{v',v'',J',J''}$ , the so-called  $gf$ -value, is plotted in Figure 2 as a function

<sup>2</sup>In atomic weight units, Aston's scale

<sup>3</sup>A discussion of the number and accuracy of the  $X \ ^2\Sigma^+$  rovibrational states is given in Skory et al. (2002).

<sup>4</sup>The complete list of MgH oscillator strength data is available online at the UGA Molecular Opacity Project database website <http://www.physast.uga.edu/ugamop/>

of the absorbed photon energy where comparison is made to the line list of Kurucz (1993a). To the best of our knowledge, the Kurucz (1993a) calculations were performed with a model rotational Hamiltonian using spectroscopic constants (Kurucz 1993b). Thus, the differences arising between both sets of results can be mainly explained by the fact that the model Hamiltonian method, though satisfactory for low-lying rovibrational levels, may lose accuracy as  $v$  and/or  $J$  increase. Further, it seems that the same  $J_{\max}$  was used for all vibrational levels (Kurucz, private communication, 2002) which is clearly not the case as shown in Table 2. This appears to explain why the band-series in the Kurucz (1993a) calculations extend to larger photon energies.

### 3.2. Atmosphere models

The models used for this work were calculated as described in Allard et al. (2001). These models and their comparisons to earlier versions are the subject of a separate publication (Allard et al. 2001) and we thus do not repeat the detailed description of the models here. However, we will briefly summarize the major physical properties. The models are based on the Ames H<sub>2</sub>O and TiO line lists by Partridge & Schwenke (1997) and Schwenke (1998) and also include as a new addition the line lists for FeH by Phillips & Davis (1993) and for VO and CrH by R. Freedman (NASA-Ames, private communication). The models account for equilibrium formation of dust and condensates and include grain opacities for 40 species. In the following, the models will be referred to as “AMES-dusty” for models in which the dust particles stay in the layers in which they have formed and “AMES-cond” for models in which the dust particles have sunk below the atmosphere from the layers in which they originally formed. We stress that large uncertainties persist in the water opacities for parts of the temperature range of this work (Allard et al. 2000). However, almost all MgH bands are in the optical and are thus affected minimally by the quality of the water opacities.

In addition to the opacity sources listed above and in Allard et al. (2001, and references therein) we added the new  $A$ - $X$  bound-bound radiative transition data from this work and the  $B'$ - $X$  and  $X$ - $X$  data from Skory et al. (2002) for all isotopes <sup>24</sup>MgH, <sup>25</sup>MgH, and <sup>26</sup>MgH to our opacity database. In order to assess the effects of the new MgH data, we compare spectra calculated with these opacity sources to spectra calculated with the MgH line data provided by Kurucz in his list of spectral lines of diatomic molecules (Kurucz 1993a). In addition, we have computed a number of models with and without MgH data. The original AMES grid was calculated for effective temperatures of M, L, and T dwarfs. The hotter models in this work are based on the same physics as the AMES grid and merely differ in the effective temperature. The models used in the following discussion were all iterated

to convergence for the parameters indicated. The high resolution spectra which have the individual opacity sources selected are calculated on top of the models. The MgH bands are too localized in a region with little flux, or too weak to influence the temperature structure of the atmosphere.

In Figure 3 we show comparisons between spectra from models using no MgH data, spectra from models using the new MgH line list and spectra from models using the Kurucz (1993a) MgH line list in the spectral region where the MgH bands are most prominent. The comparisons have been done at effective temperatures of 2000 K, 3000 K, and 4000 K to sample the temperature range in which MgH is visible in the spectrum. For convenience, we only did the comparison for models with  $\log(g)=5.0$ . As can be seen, the Kurucz (1993a) line lists overestimates the opacity due to the inclusion of non-existent levels with high  $J$ -values and the use of a model Hamiltonian approach. The differences between the spectra with the new and Kurucz (1993a) MgH line lists are very similar for the AMES-Cond and AMES-Dusty models although the overall flux level and the overall flux shape are different for AMES-Cond and AMES-Dusty in the optical (Note that reversing the 1.0 dex offset applied in the plot is not sufficient to match the two 2000 K models). Another view is presented in figure 4 which shows the relative difference in the spectra. As can be seen, there are significant differences spreading among both the  $A - X$  and the  $B' - X$  transitions.

Since the MgH data presented by (Kurucz 1993a) was intended for solar-type stars we also compared the resulting spectra for an effective temperature of 5800 K and  $\log(g)=4.5$ , relevant parameters for solar-type stars. As can be seen as part of Figure 4, the differences are negligible. Although the effect of the non-existent levels with high  $J$ -values should be more important for hotter temperatures, the decrease in the abundance of MgH at higher temperatures makes the effect unobservable. Finally, we want to note that for the 2000 K AMES-Cond model the X-X band adds a small amount of opacity at around  $4\mu\text{m}$  and  $10\mu\text{m}$ .

#### 4. Conclusion

Using a combination of theoretical and experimental data on the potential energies and dipole transition moment of MgH, a comprehensive theoretical vibrational-rotational line list for the  $A \ ^2\Pi \leftarrow X \ ^2\Sigma^+$  transition was constructed. When using the new  $A \leftarrow X$  line data and the new  $B' \ ^2\Sigma^+ \leftarrow X \ ^2\Sigma^+$  and the  $X \ ^2\Sigma^+ \leftarrow X \ ^2\Sigma^+$  line data of Skory et al. (2002) in synthetic spectrum calculations, we find significant differences in the opacity when comparing the spectra to calculations using the existing data of Kurucz (1993a). The differences are largest for effective temperatures pertaining to L and M type stars and can easily be seen in low resolution work. For hotter stars, of K and G type, the differences are



less pronounced and high resolution spectra are required to notice the improvements for the hottest stars.

This work was supported in part by NSF grants AST-9720704 and AST-0086246, NASA grants NAG5-8425, NAG5-9222, and NAG5-10551 as well as NASA/JPL grant 961582 to the University of Georgia. This work also was supported in part by the Pôle Scientifique de Modélisation Numérique at ENS-Lyon. Some of the calculations presented in this paper were performed on the IBM SP2 and the SGI Origin of the UGA EITS, on the IBM SP “Blue Horizon” of the San Diego Supercomputer Center (SDSC), with support from the National Science Foundation, and on the IBM SP of the NERSC with support from the DoE. We thank all these institutions for a generous allocation of computer time. We thank Stephen Skory for assistance during the early part of this work. P.F.W. and K.K. are grateful to B. Kurucz for useful discussions.

## REFERENCES

- Allard F., Hauschildt P. H., Alexander D. R., Tamanai A., Schweitzer A., 2001, *ApJ*, 556, 357
- Allard F., Hauschildt P. H., Schweitzer A., 2000, *ApJ*, 539, 366
- Balfour, W. J., & Cartwright, H. M. 1976, *A&AS*, 26, 389
- Balfour, W. J., & Lindgren, B. 1978, *Can. J. Phys.*, 56, 767
- Bernath, P. F., Black, J. H., & Brault, J. W. 1985, *ApJ*, 298, 375
- Bonnell, J. T. & Bell, R. A. 1993, *MNRAS*, 264, 334
- Cooley, J. W. 1961, *Math. Computation*, 15, 363
- Gay, P. L. & Lambert, D. L. 2000, *ApJ*, 533, 260
- Herzberg, G. 1950, *Molecular Spectra and Molecular Structure, Vol. I, Spectra of Diatomic Molecules* (Princeton: D. Van Nostrand)
- Huber, K. P. & Herzberg, G. 1979, *Molecular Spectra and Molecular Structure, Vol. IV, Constants of Diatomic Molecules* (New York: Van Nostrand Reinhold)
- Kirby, K., Saxon, R. P., & Liu, B. 1979, *ApJ*, 231, 637

- Kurucz, R. L. 1993a, CD-ROM No.15 Diatomic molecular data for opacity calculations (Harvard-Smithsonian Center for Astrophysics)
- Kurucz, R. L. 1993b, *Molecules in the Stellar Environment*, ed. U. G. Jørgensen (Berlin: Springer-Verlag), p. 282
- Larsson, M. 1983, *A&A*, 128, 291
- Majewski, S. R., Ostheimer, J. C., Kunkel, W. E., & Patterson, R. J. 2000, *AJ*, 120, 2550
- NIST Atomic Spectra Database 1999, [http://aeldata.phy.nist.gov/cgi-bin/AtData/main\\_asd](http://aeldata.phy.nist.gov/cgi-bin/AtData/main_asd)
- Partridge H., Schwenke D. W., 1997, *J. Chem. Phys.*, 106, 4618
- Phillips J. G., Davis S. P., 1993, *ApJ*, 409, 860
- Reid, I. N., Kirkpatrick, J. D., Gizis, J. E., Dahn, C. C., Monet, D. G., Williams, R. J., Liebert, J., & Burgasser, A. J. 2000, *AJ*, 119, 369
- Saxon, R. P., Kirby, K., & Liu, B. 1978, *J. Chem. Phys.*, 12, 5301
- Schwenke D. W., 1998, *Chemistry and Physics of Molecules and Grains in Space. Faraday Discussion*, 109, 321
- Skory, S., Stancil, P. C., Weck, P. F., & Kirby, K. 2002, *ApJS*, in preparation
- Sotirovski, S. 1972, *A&AS*, 6, 85
- Standard, J. M., & Certain, P. R. 1985, *J. Chem. Phys.*, 83, 3002
- Wallace, L., Hinkle, K., Li, G., & Bernath, P. 1999, *ApJ*, 524, 454
- Whiting, E. E., & Nicholls, R. W. 1974, *ApJS*, 27, 1

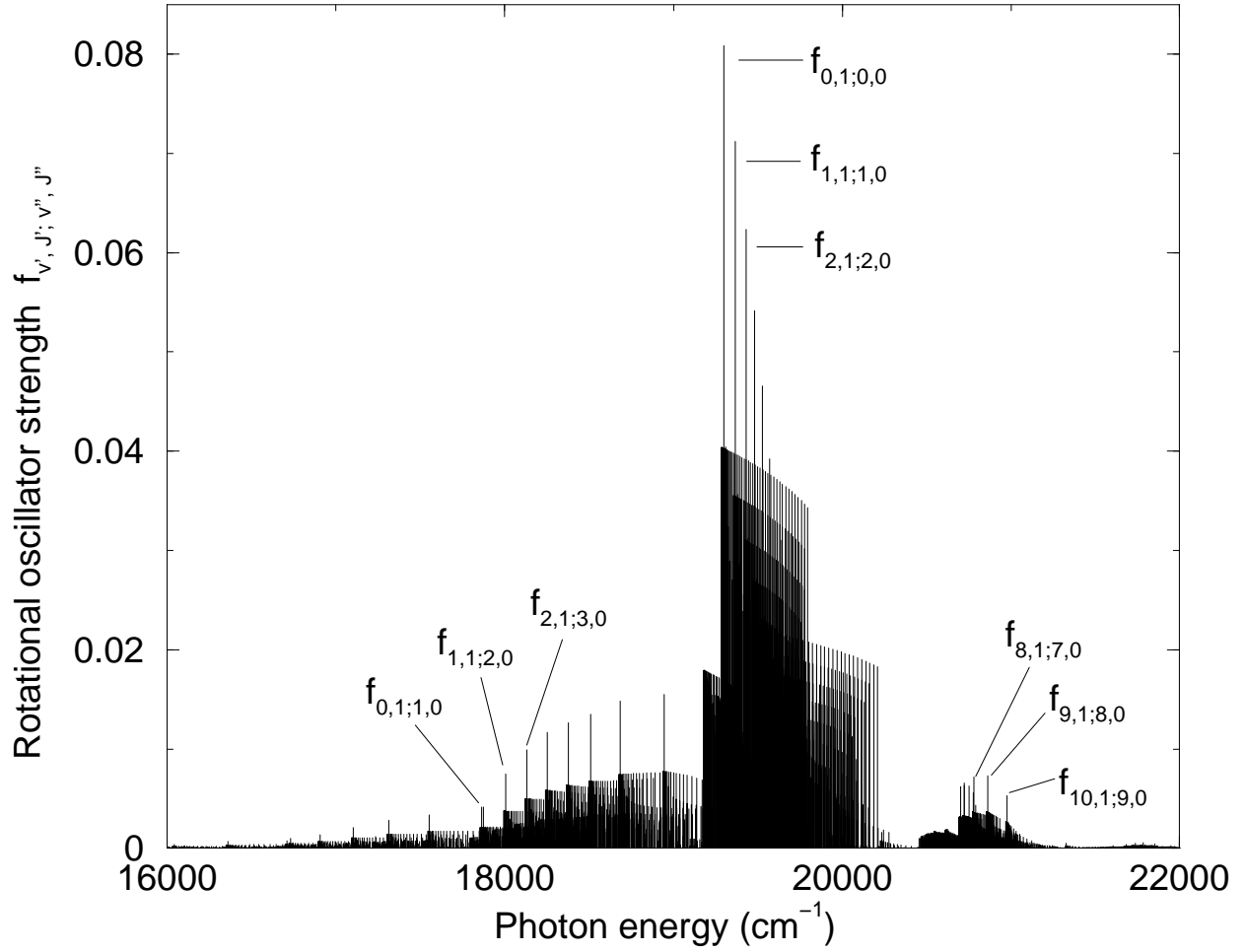


Fig. 1.— Rotational oscillator strengths  $f_{v', J'; v'', J''}$  as a function of wavelength of the absorbed photon energy.

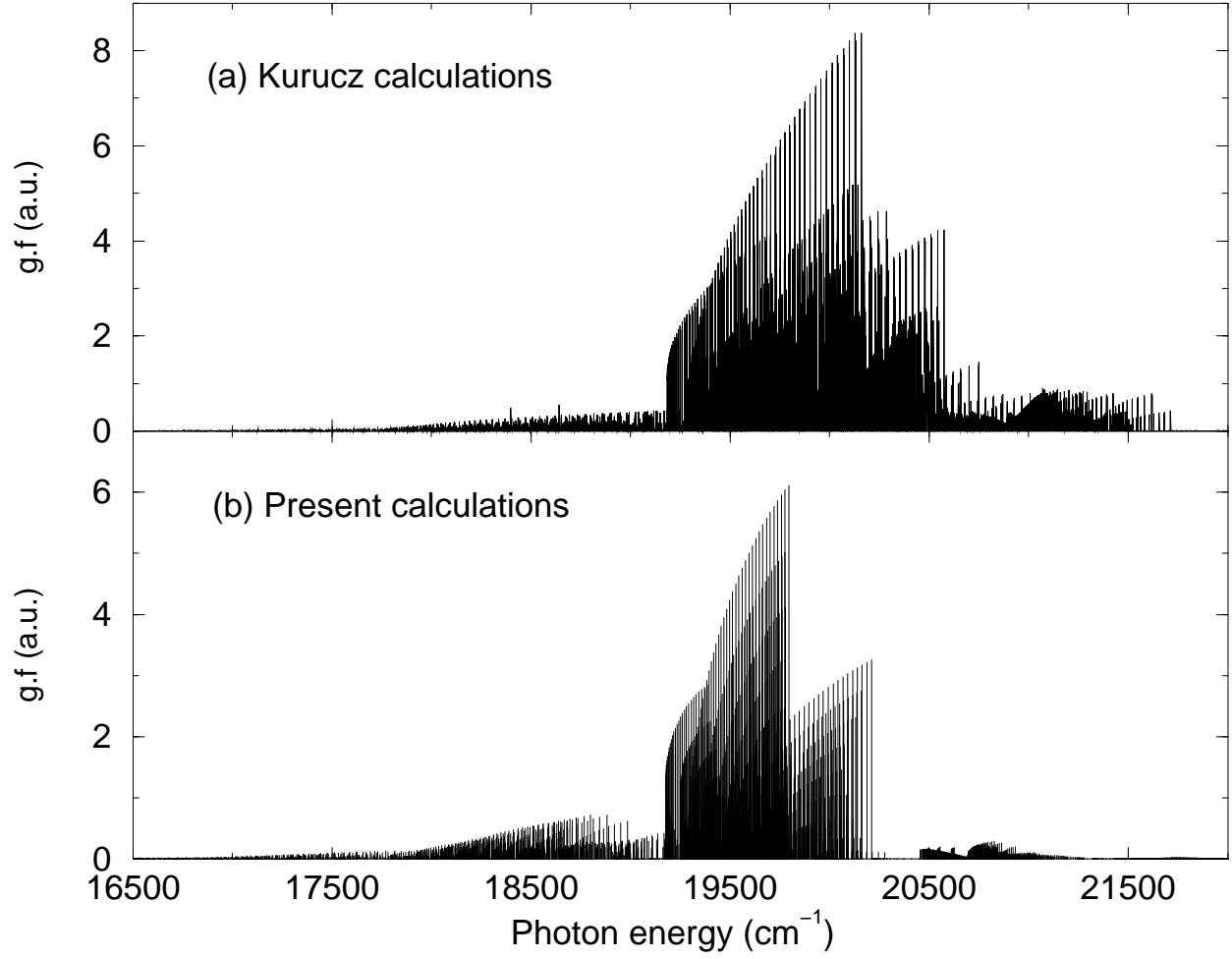


Fig. 2.—  $g_{J',J''} \cdot f_{v',v'',J',J''}$  values as a function of the absorbed photon energy. (a) calculations of Kurucz (1993a); (b) present calculations.

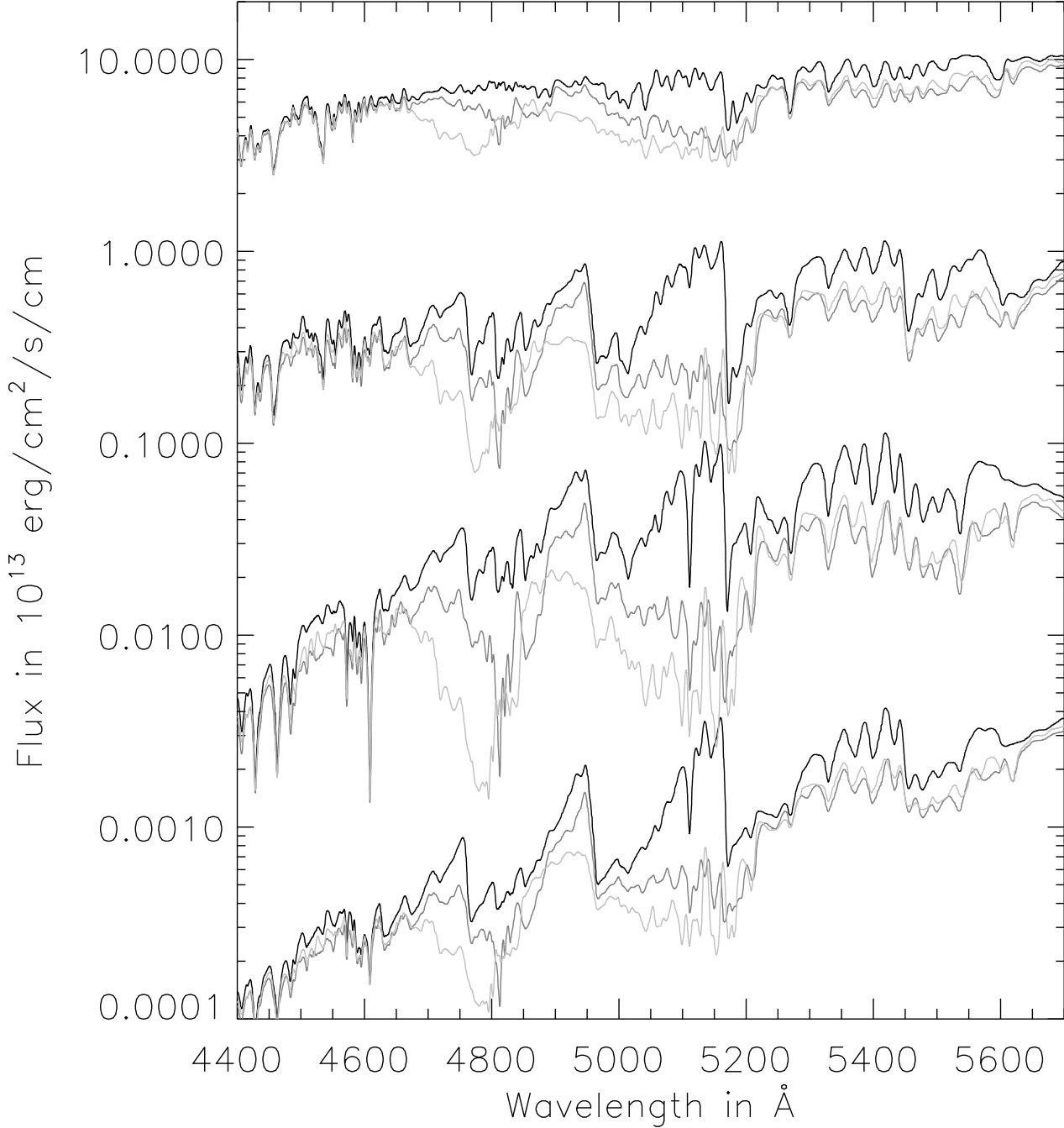


Fig. 3.— Spectra of the strongest MgH bands for models with  $T_{\text{eff}}=4000$  K,  $T_{\text{eff}}=3000$  K,  $T_{\text{eff}}=2000$  K (AMES-Cond model) and  $T_{\text{eff}}=2000$  K (AMES-Dusty model) (from top to bottom). The 2000 K AMES-Cond models have an artificial offset of +1.0 dex for better legibility. All models have  $\log(g)=5.0$  and are AMES-Cond unless noted otherwise. The black spectra are from models without MgH data, the dark grey spectra are from models with the new MgH data and the light grey spectra are from models using the Kurucz (1993a) MgH data. The resolution of the calculated spectra are much higher. For illustrative purposes the spectra have been reduced to a resolution of  $R=80$  at  $5000 \text{ \AA}$ .

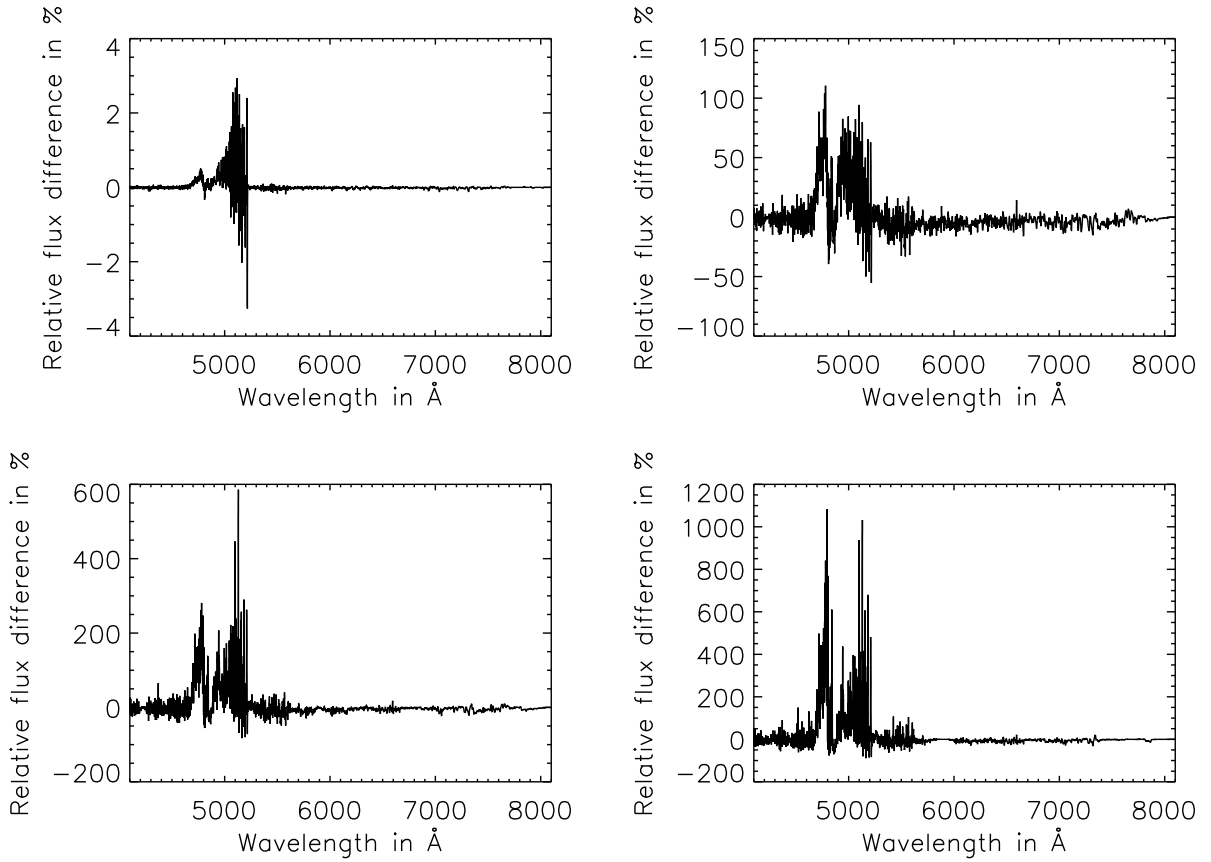


Fig. 4.— Relative flux differences between models when changing from the Kurucz (1993a) MgH data to the new MgH data. The models are from top left to bottom right 5800 K, 4000 K, 3000 K and 2000 K. All models are AMES-Cond and have  $\log(g)=5.0$ , except the 5800 K model has  $\log(g)=4.5$ . The resolution of all spectra have been reduced to  $R=500$  before calculating the ratio.

Table 1. Asymptotic Separated-Atom and United-Atom Limits

Molecular State	Atomic States	Separated-Atom			C <sub>6</sub>	C <sub>8</sub>	C <sub>10</sub>	United Atom (Al)
		Energy (eV)						
		Theory	Expt					
$X \ ^2\Sigma^+$	Mg( $3s^2 \ ^1S$ )+H( $1s \ ^2S$ )	0.0	0.0	57.8 <sup>a</sup>	2490 <sup>b</sup>	115000 <sup>b</sup>	$3s^2 3p \ ^2P^0$	
$A \ ^2\Pi$	Mg( $3s3p \ ^3P^0$ )+H( $1s \ ^2S$ )	2.596	2.714 <sup>c</sup>	56.9 <sup>d</sup>	2451 <sup>d</sup>	113205 <sup>d</sup>	$3s^2 3p \ ^2P^0$	
$B' \ ^2\Sigma^+$	Mg( $3s3p \ ^3P^0$ )+H( $1s \ ^2S$ )	2.593	2.714 <sup>c</sup>	56.9 <sup>d</sup>	2451 <sup>d</sup>	113205 <sup>d</sup>	$3s^2 4s \ ^2S$	

<sup>a</sup>A. Derevianko (private communication, 2001).

<sup>b</sup>From Standard & Certain (1985).

<sup>c</sup>Weighted average of the  $^3P_0$ ,  $^3P_1$ , and  $^3P_2$  term energies from NIST Atomic Spectra Database (1999).

<sup>d</sup>Estimate, Skory et al. (2002).

Table 2. Vibrational binding energies<sup>a</sup> and  $\Delta G(v' + 1/2)$  in  $\text{cm}^{-1}$  for the  $A\ ^2\Pi$  state

$v'$	$J'_{max}$	B. E. <sup>b</sup>	$\Delta G(v' + 1/2)$		
			Theory <sup>b</sup>	Saxon <sup>c</sup>	Expt. <sup>d</sup>
0	49	12903.7	1494.3	1493.9	1533.9
1	47	11409.4	1423.2	1423.2	1466.1
2	44	9986.2	1349.0	1349.5	1394.4
3	42	8637.2	1273.2	1273.0	...
4	39	7364.0	1196.4	1191.8	...
5	36	6167.5	1132.0	1103.9	...
6	33	5035.5	1082.9	1007.4	...
7	30	3952.6	1013.1	900.2	...
8	27	2939.5	905.7	780.2	...
9	23	2033.8	744.7	645.7	...
10	19	1289.1	573.3	495.0	...
11	15	715.8	414.1	330.9	...
12	11	301.8	170.1	...	...
13	6	131.7	...	...	...

<sup>a</sup>Binding energies are given for rotationless vibrational levels

<sup>b</sup>This work

<sup>c</sup>Saxon et al. (1978)

<sup>d</sup>Balfour & Cartwright (1976)



Table 3. Band oscillator strengths\* and transitions energies† for the  $A\ ^2\Pi \leftarrow X\ ^2\Sigma^+$  Band System

$v'$ ( $A^2\Pi$ )	$(X^2\Sigma^+) v'' = 0$		$v'' = 1$		$v'' = 2$		$v'' = 3$	
	$E_{v'0}$	$f_{v'0}$	$E_{v'1}$	$f_{v'1}$	$E_{v'2}$	$f_{v'2}$	$E_{v'3}$	$f_{v'3}$
0.....	19290	1.616(-1)	17867	8.30(-3)	16506	5.2(-4)	15209	4.1(-5)
	19292	1.61(-1)	17860	8.61(-3)	16492	5.3(-4)	15190	4.1(-5)
1.....	20784	4.88(-3)	19361	1.424(-1)	18000	1.49(-2)	16702	1.48(-3)
	20826	5.14(-3)	19394	1.41(-1)	18025	1.59(-2)	16724	1.52(-3)
2.....	22207	1.0(-5)	20784	8.62(-3)	19422	1.246(-1)	18125	1.99(-2)
	22288	3.9(-6)	20856	9.38(-3)	19490	1.24(-1)	18185	1.99(-2)
3.....	23555	6.9(-7)	22132	5.9(-5)	20770	1.11(-2)	19473	1.082(-1)
	23682	4(-7)	22250	4.4(-5)	20884	1.14(-2)	19579	1.09(-1)
4.....	24828	1.4(-8)	23405	2.2(-6)	22043	2.0(-4)	20747	1.25(-2)
	25002	< 1.0(-7)	23570	7.0(-6)	22204	2.4(-4)	20899	1.27(-2)
5.....	26024	1.3(-9)	24601	1.3(-7)	23240	2.8(-6)	21943	5.0(-4)
	26243	< 1.0(-7)	24811	< 1.0(-7)	23445	5.0(-6)	22140	5.2(-4)
6.....	27156	1.2(-9)	25733	8.7(-9)	24371	6.5(-7)	23074	1.2(-6)
	27398	< 1.0(-7)	25966	4.0(-7)	24600	2.0(-6)	23295	1.0(-6)

\*Band oscillator strengths are given in a.u. and are calculated for rotational quantum numbers  $J'' = 0$  and  $J' = 1$ . Our results are listed on the first line, with the previous calculations of Kirby et al. (1979) below. Notation:  $x(-n) \equiv x \times 10^{-n}$

†Energies  $E_{v'v''}$  of the absorbed photon are given in  $\text{cm}^{-1}$ . Our values are listed on the first line, with the experimental transition energies given by Balfour & Cartwright (1976) below (generally as listed in Kirby et al. (1979)), for  $J'' = 0$  and  $J' = 1$ .